ON SCALING OF THE MAXIMUM ICE PRESSURE ON A VERTICAL FOUNDATION

Lennart Fransson and Thomas Olofsson
Luleå University of Technology
Sweden

ABSTRACT

The nature of ice loads on vertical foundations is discussed based on statistical analysis of field data. Measured loads on segments of the total pressure area were typically Weibull distributed with a maximum of about 4 times the mean values. Scale effect on the maximum effective pressure was evident for uniform level ice when calculated for different contact widths. Maximum pressure on a larger contact width decreased but the mean pressure level remained constant. This confirmed the assumption that some but not all of the governing crushing phenomena were statistically independent. Elasticity of the structure or the ice sheet was assumed to increase the length of the independent crushing zones.

ICE EDGE CRUSHING AND SCALING

Average ice pressure on different contact areas can be calculated from simultaneous load measurements on vertical segments of a structure. In this study the measured loads were associated with brittle crushing at the contact with the segments. According to Bazant (2002) scaling of strength (not only for brittle materials) is supported by at least three different theories. Weibull statistical theory of random strength (Weibull, 1939) is classical in solid mechanics. Secondly there is the theory of stress redistribution and fracture energy release caused by large cracks and thirdly the theory of crack fractality. Application of linear elastic fracture mechanics results in a strong size effect, which have been verified in experimental studies in the range 3m-80m for sea ice (Dempsey et al., 1995). It is truly an empirical finding that measured ice pressure on structures decreases with area (Sanderson, 1988) and many explanations for this phenomenon have been proposed. The assumption of a strong scale effect in compressive strength (Gershunov, 1986) can however be misleading because ice sheets are extremely brittle. In fact continuous ice crushing of ice sheets against a structure seems to have very little in common with standardized strength

testing. Several intricate processes other than compression of ice take place separately or parallel in connection with ice edge crushing:

1. Flaking, pulverisation and similar types of fine-grained fracturing.
2. Extrusion of crushed and compressed ice and water.
3. Formation of large cracks parallel with the surface of the ice sheet.
4. Sudden instability failures (buckling) of cracked ice.

In addition, many of the crushing processes occur nonsimultaneous along the contact width. Pressure associated with (1) and (2) probably oscillates at different frequencies and amplitudes than (3) and (4), but identification of processes based on load measurements on a large contact area seems impossible. Ice crushing at high speed and with a stiff ice/structure system tends to reduce the size of the cracks. When the velocity of the ice sheet is about 0.1 m/s brittle crushing and buckling take place. In this case and in all ice/structure interactions the ratio between structure width and ice thickness is important. At a high aspect ratio buckling is more likely to limit the maximum effective pressure. Size effect on brittle fracturing also implies that the effective pressure decreases with ice thickness as long as the aspect ratio is held constant. This interesting question is however left out from the discussion. Without knowing the actual type of ice crushing process, simple statistical methods can be used to describe the time series of the registered ice loads. Simultaneous registration of loads at multiple segments of a structure adds important information on the scale effect. According to the central limit theorem we should expect a normal distribution with a small standard deviation when many segment pressures are summed up if ice crushing on different segments is statistically independent.

Kry (1978) first made the assumption of independent ice failure zones, which he believed was valid only for wide structures. Independent zones should be wider than the largest pieces of fractured ice on a very wide structure. Kry summed up simulated log-normal pressure distributions on such zones which resulted in a reduction of the design pressure as a function of number of zones. This type of size effect and other statistical properties of the field data from the lighthouse Norströmsgrund have been studied in the EU-project LOLEIF. The same statistical approach has also been applied on data from ice edge crushing with two small segmented indentors and these results have been compared with the results from Norströmsgrund.

EVENT 0303_022 AT LIGHTHOUSE NORSTRÖMSGRUND

In the EU-project LOLEIF (1998-2000) ice pressures were measured on 9 of totally 20 segments around the perimeter of the Swedish lighthouse Norströmsgrund in the Gulf of Bothnia. In this study the ice crushing event 0303_022 was chosen because the interacting ice thickness was fairly constant with a mean thickness of 0.26 m. Observed vibrations associated with this event were small and possibly insignificant

for the ice load development. The design of the data acquisition system (parallel A/D converters) made it possible to register all loads simultaneously with a high degree of accuracy. In the chosen event, 16 synchronized loads were registered for 20 minutes with a sampling rate of 30 Hz. Important details about the actual loading scenario and geometry of load sensors are shown in Fig.1, Tables 1 and 2.

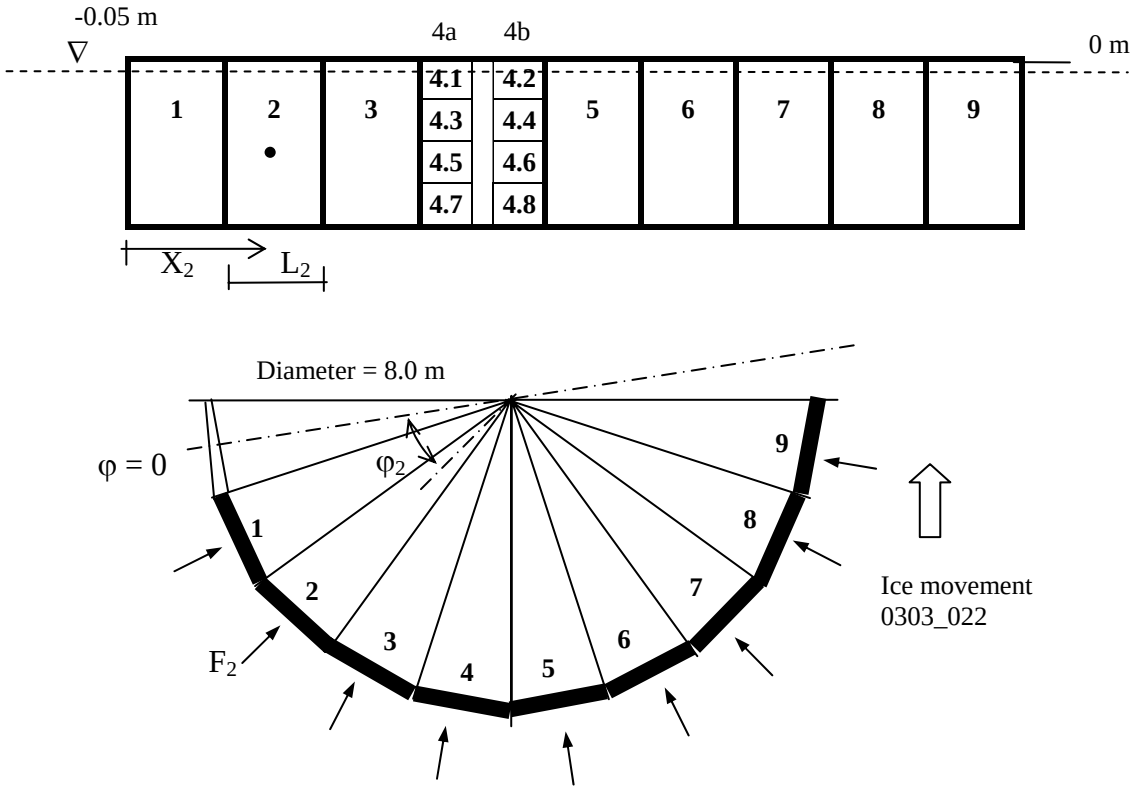

Fig. 1. Lay-out of pressure sensors and geometry of the segmented lighthouse foundation. Segment 4 was divided into 8 smaller sensors (4.1-4.8).

Table 1. Ice data

0303_022 Date	Water level[1] (m)	Ice thickness[2] h (m)	Ice speed[3] v (ms^{-1})	Ice move direction[3] θ (π/10)	Wind speed (ms^{-1})	Air temp (°C)	Ice properties[4]		
							Ice type	Salinity (ppt)	Strength (MPa)
2000-03-03	-0.05	0.26 ± 0.04	0.20	4 ½	8	-8	Level ice	0.6	1.1-1.4

[1] Relative to upper edge of load sensors, [2] Registration (0.14 Hz) with sonar, [3] Estimation from video recordings, [4] Field tests 2000-03-22, compressive load applied on samples cut from the ice sheet

Table 2. Summary of segment loads.

0303_022 Segment	Reg. Length L (m)	Centre Line X (m)	Reg. Angle φ (π/10)	Mean Pressure (kNm^{-1})	Max Pressure (kNm^{-1})	Standard Dev (kNm^{-1})	Skew-ness	Remarks:
1	1.21	0.605	1	125	372	50	0.43	
2	1.21	1.865	2	119	361	54	0.70	
3	1.21	3.125	3	111	414	56	0.44	
4a	0.50	4.030	4	111	478	58	0.83	4.1 + 4.3 + 4.5 + 4.7
4b	0.50	4.740	4	114	499	62	0.68	4.2 + 4.4 + 4.6 + 4.8
4	1.00	4.385	4	112	412	50	0.44	4a + 4b
5	1.21	5.645	5	107	401	59	0.56	
6	1.21	6.905	6	108	377	59	0.54	
7	1.21	8.165	7	103	161	27		partially out of order
8	1.21	9.425	8	139	410	60	0.22	
9	1.21	10.685	9	111	297	47	0.09	

MEASURED CRUSHING PRESSURE

Ice pressure p as a function of time t is here defined

$$p(t) = \frac{F(t)}{L} \qquad (1)$$

where $F(t)$ is the registered load normal to the segment and L is the corresponding registration length defined in Fig. 1. When the total load on two or more adjacent segments were considered L was the total registration length. The probability density functions of individual segment pressures, shown in Fig. 2, were of Weibull type with maximum pressures of about four times the mean level. The skewness was typically greater than 0.4, see Table 2. It can be seen from the graph that the measurement at segment 7 differs from other segments probably due to a frozen load panel. Segment 7 was therefore omitted in further analysis.

Pressure variation on individual segments was in general more dynamic than pressure on the total structure. The maximum pressure decreased substantially with increasing registration length whereas the mean pressure was constant. It can be noticed that the mean pressure level dropped several times over a period of 20 minutes. From video recordings it was observed that the mean pressure drops were caused by large instability failures of the ice sheet in front of the structure. Pressure variations on segment 1 and on the total registration length are shown in Fig. 3.

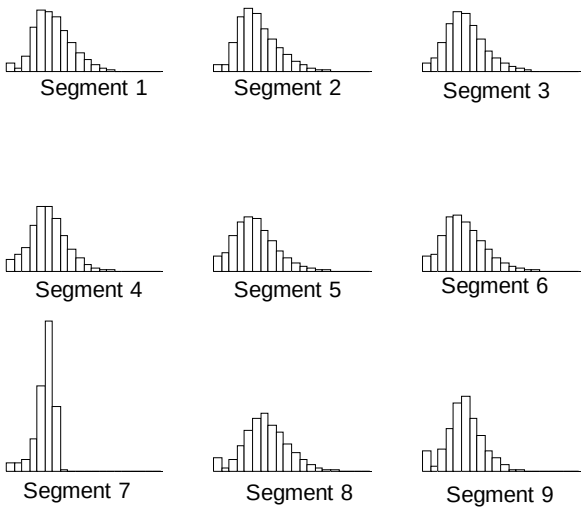

Fig. 2. Probability density functions for segment pressures (0-414 kNm^{-1}).

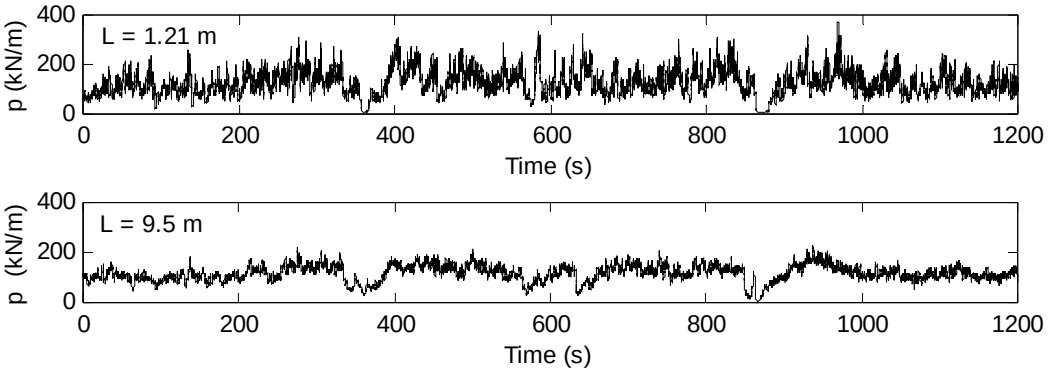

Fig. 3. Pressure variation on segment 1 (L=1.21 m) and on the total registration length (L=9.5 m).

Statistical properties of ice pressure on different segments were relatively independent of registration angle φ as long as the whole segment was involved in ice crushing. Fig. 4 shows segment pressures vs. position on the fundament. Mean pressure was almost constant at all segments with some minor peaks at segments 1 and 8. Segment 9 appeared to be at the end of the crushing zone and the maximum pressure was somewhat lower than for the rest of the segments. Nevertheless, segment 9 was incorporated in the analysis although it might have caused some extra scatter in the result. The evaluation of scale effects was however deemed to be relatively unaffected by the slightly different load history on the end segments.

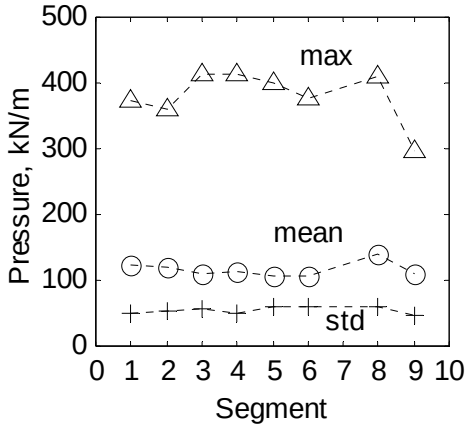

Fig.4. Spatial distribution of pressure on segments. Maximum (Δ), Standard Deviation (+), Mean (o).

SCALING OF PRESSURE

Three basic statistical properties of measured ice pressures have been studied, namely maximum, standard deviation and mean pressure level. Power scaling was assumed for all these properties and L/L_0 was used as the dimensionless scaling ratio.

Maximum pressure: $$p^{\max} = p_0\left(\frac{L}{L_0}\right)^{\alpha} \quad (2)$$

Standard deviation: $$s = s_0\left(\frac{L}{L_0}\right)^{\beta} \quad (3)$$

Mean pressure: $$\mu = \mu_0\left(\frac{L}{L_0}\right)^{\gamma} \quad (4)$$

α, β and γ are the scale exponents and p_0, s_0 and μ_0 are nominal values scaled to the reference length L_0. In this study the reference length L_0 was set equal to the average ice thickness h. Pressure lengths were in the interval 0.5m – 10m, see Table 3, and the ice thickness in event 0303_022 was 0.26m. Consequently, segment pressures were registered on a length that always was greater than the ice thickness which means that the expected pressure on L = h had to be extrapolated. Assuming a normal pressure distribution $\beta = -0.5$ indicates that the segment pressures on actual

segment lengths are independent. A consistently skew distribution or periods of correlated segment pressures results in $-0.5 < \beta < 0$.

Maximum, mean and standard deviation were calculated for single segments and sets of adjacent segments and plotted as a function of scale L/h. The obtained scale effects are shown as straight lines in the log-log diagram in Fig. 5.

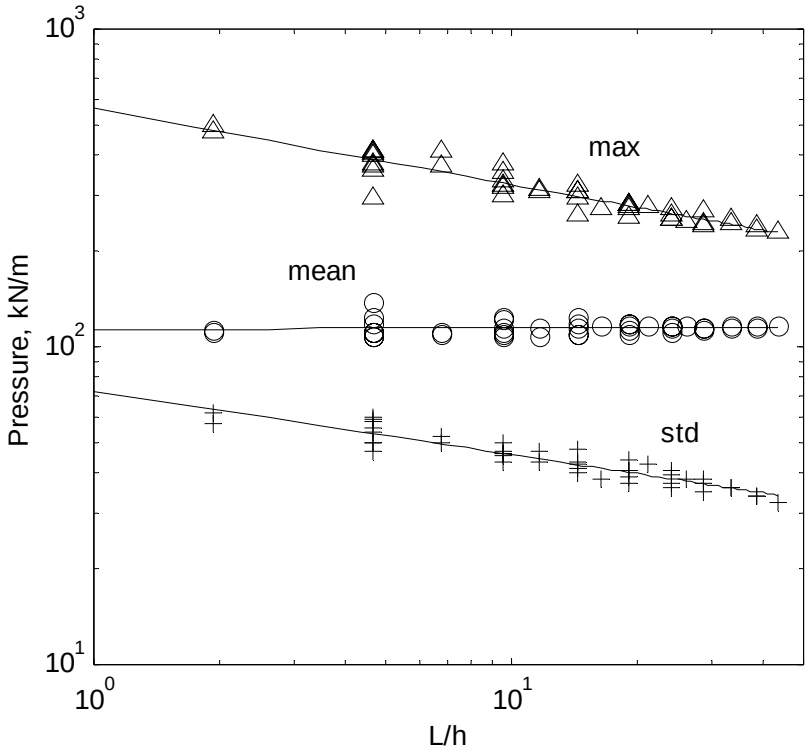

Fig. 5. Scale effect based on summation of adjacent segment loads divided with their total registration length. Maximum (Δ), Standard Deviation (+), Mean (o). Best fit for 45 legal combinations was obtained with the exponents α = -0.24, β = -0.20 and γ = 0.0054.

With a skew distribution there is no simple method to predict extreme values. The rule of $p^{max} \approx \mu + 3s$ used for a normal distribution doesn't work. Maximum pressure on individual segments was much higher than the mean pressure but the events were rare. A long sampling time was needed to catch the extremes. This method to study scale effect on ice pressure involve a summation of correlated and uncorrelated pressures resulting in a transformation of the probability density function. Measurements of loads from many uncorrelated segments resulted in a normal distribution of the total pressure. When approaching the normal distribution

(L > 10 h) the maximum pressure was a well-defined function of the standard deviation. On the other hand measurements on individual segments (L < 5h) were not well described with the evaluated standard deviation. Based on these observations an exponential equation to fit the data was proposed. Maximum pressure is then calculated from the scale dependent standard deviation as

$$p^{\max} = a_0 \mu_0 \exp(k \; s / \mu_0) \qquad (5)$$

The constants a_0 and k can be obtained from crushing tests where scale effects are evident. It was hard to find digital raw-data from brittle crushing tests with stiff segmented structures but two other cases have been analysed and compared with the full-scale data. The result is given in Table 3.

Table 3. Scale properties obtained from ice crushing tests with segmented structures.

Test data	Structure width D (m)	Ice thickness h (m)	Velocity v (m/s)	Rec. time T (s)	Aspect ratio D/h	Mean effective pressure μ_0/h (MPa)	Max pressure p_0/μ_0	Standard deviation s_0/μ_0	Scale exponent Eq. (2) α	Scale exponent Eq. (3) β	Coeff. in Eq.(5) a_0	k
a	0.4	0.20	0.7	0.5	2.0	3.1	1.6	0.21	-0.25	-0.50	0.94	2.42
b	0.25	0.033	0.1	1	7.6	1.0	3.2	0.50	-0.1	-0.3	2.17	0.83
c	8.0	0.26	0.2	1200	31	0.44	4.9	0.64	-0.24	-0.20	0.93	2.72

a) Flat indentor with 4 segments pushed by an icebreaker in fresh-water ice, Fransson (1995). Loads from raw data scanned at 1 kHz,

b) Flat indentor with 5 segments pushed by a screw-driven carriage. Laboratory tests on seeded fresh-water ice in a basin, Sodhi (1998). Data were extracted from the digitally published figures of Test #582 using image analysis.

c) Lighthouse foundation in moving sea ice. Event 0303_022 described in this paper.

The fine-grained ice crushing in test (a) fitted well to a normal distribution with the scale exponent $\beta = -0.5$. Test (b) was scattered (extracted data from the journal may have been distorted) but mean and max pressure was about the same as reported by Sodhi (1978). Individual pressures as well as average pressure on all segments fitted well into the Weibull distribution. This was verified with original graphs provided by Dr. Sodhi. Standard deviation for mean effective pressure given in Table 3 was less than 10%, which indicates that pressure was relatively insensitive to end effects. From this follows that no scale effect could be traced on the mean pressure ($\gamma \approx 0$).

Despite the fact that data sets (a) and (b) have too short recording times and small segments, scale effects were comparable. One striking difference is that the mean pressure level decreases drastically with increasing aspect ratio, see Fig. 6. Max pressure showed a similar trend but the span between max and mean pressure was larger when the measurement was done on a wide structure.

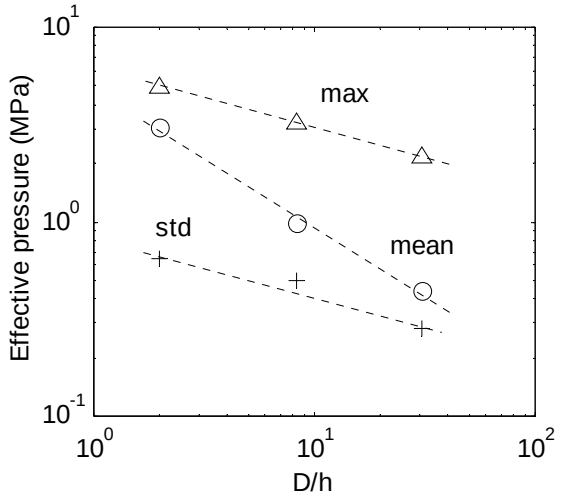

Fig. 6. Effective pressure vs. aspect ratio D/h. The result was obtained from the cases (a), (b) and (c) shown in Table 3.

CORRELATION COEFFICIENT

The correlation coefficient (corrcoef) for pairs of segment pressures is believed to be dependent on the distance *X* between the observation points as shown by Sodhi (1998). Sensors with a short measuring length *L* are likely to be less correlated than wide sensors and the stiffness of the sensors must be comparable. The registration length was usually the same for compared sensors, otherwise the average registration length was used. Correlation coefficients of the three datasets described in Table 3 are shown in Fig. 7. Corrcoef = 1 means that the segment pressures are linearly dependent on each other. Segment pressures in test (a) were on average uncorrelated with corrcoef close to zero. Indentor ends showed anti-correlation which may have been a result of the short indentation distance. Segments in test (b) were somewhat more correlated with $0 <$ corrcoef < 0.5. The original (b) data showed a similar trend as for (c) where the correlation coefficient decreases slowly from 0.5 to a level of 0.2. It is interesting to note that the assumption of independent crushing zones is applicable in case (a) for zones that are smaller than the ice thickness.

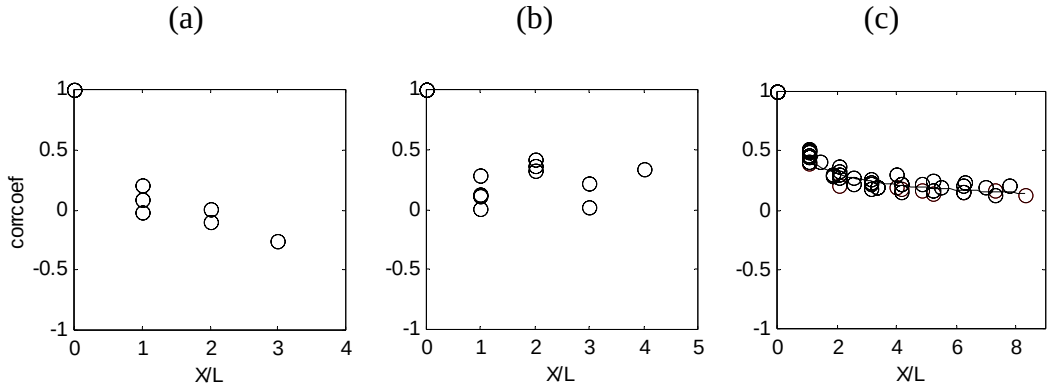

Fig. 7. Correlation coefficients of pair of segment pressures vs. relative distance. L=0.1m (a), L=0.05m (b), L=0.5m or 1.21 m (c).

DISCUSSION AND CONCLUSIONS

The obtained segment pressures depict typical crushing behaviour for level ice on a given structure. Power scaling was applicable on the maximum as well as on the standard deviation of obtained pressures. In a more advanced analysis the assumption of distribution and statistical laws could be used to predict the scaling. Several parameters were assumed to stay constant under the studied period such as the ice properties and the velocity of the ice sheet. This was obviously a coarse approximation that became worse as the time span was increased. On the other hand a too short time span may lead to underestimation of the maximum pressure. Synchronized data on the ice thickness was available and can be used to refine the analysis. Variation of ice properties was however only partly reflected by the ice thickness. Cracks and inhomogeneity also varied along the studied distance (240 m) for this type of moving sea ice. Pressures averaged for about 10 seconds could eventually serve as a measure of the overall consistently of the ice properties. Seen over the total period of 20 minutes, mean pressures were nearly the same on all segments involved in ice crushing. Nevertheless end effects and 3-D effects due to the cylindrical shape certainly had some impact on the statistical properties. Adjacent flat segments on a cylinder are possibly more independent than segments on a flat wall or curved segments on a cylinder. If so, vertical structures can be designed in such a way that more independent crushing zones are promoted.

The concept of independent crushing zones is based on the assumption that elastic displacement of the structure or the ice sheet is negligible. Ice-induced vibration is an example of the opposite when the elastic displacement of the structure results in time correlated pressure variations (saw-tooth curves) along the ice-structure contact. The size and shape of fractured ice and thus the width of independent

crushing zones is believed to be smaller than the ice thickness as long as the ice sheet and the structure are stiff compared to the crushing zones. Otherwise load from a damaged zone is transferred to the adjacent zones. Elastic displacement of the ice sheet is more likely to occur when the aspect ratio is high. Elastic buckling without failures might have been one important source of compliance in the studied event at the lighthouse.

Scale effects obtained from measurements on one type of segmented structure cannot directly be applied on structures with other widths and stiffness. The influence of aspect ratio, ice properties and compliance of the ice/structure system are equally important to understand.

REFERENCES

Bazant, ZP (2002) Scaling of structural strength. Hermes Penton Ltd.

Dempsey JP, Adamson RM and Mulmule SV (1995) Large-scale-in-situ fracture of ice. Proc., 2nd Int. Conf. on Fracture Mech. of Concrete Structures held in Zürich, ed. by Wittmann FH, Aedificatio Publishers, Freiburg, 575-684.

Fransson L (1995) Ice load on structures – Ice testing in Luleå Harbour 1993. Coldtech Report 1995:06, Division of Structural Eng., Luleå University of Tech., Sweden.

Gershunov, EM (1986) Scale effect in ice. Cold Regions Sci. and Tech. 12 (1986) 277-284.

Kry, PR (1978) A statistical prediction of effective ice crushing stresses on wide structures. The 5th IAHR-Symposium on Ice Problems held in Luleå, Sweden 7-9 August 1978. Part 1, 33-47.

Sanderson, TJO (1988) Ice Mechanics. Risk to offshore structures, Graham and Trotman Ltd.

Sodhi DS (1998) Nonsimultaneous crushing during edge indentation of freshwater ice sheets. Cold Regions Sci. and Tech. 27 (1998) 179-195.

Weibull, W (1939) The phenomenon of rupture in solids. Proc., Royal Swedish Institute of Engineering Research 153, Stockholm.